NATIONAL ADVISORY COMMITTEE FOR AERONAUTICS

TECHNICAL NOTE 2524

AN INVESTIGATION OF AIRCRAFT HEATERS

XXXVIII - DETERMINATION OF THERMAL PERFORMANCE OF RECTANGULAR- AND TRAPEZOIDAL-SHAPED INNER-SKIN PASSAGES FOR ANTI-ICING SYSTEMS

By L. M. K. Boelter, V. D. Sanders, and F. E. Romie

University of California

Washington

November 1951

NATIONAL ADVISORY COMMITTEE FOR AERONAUTICS

TECHNICAL NOTE 2524

AN INVESTIGATION OF AIRCRAFT HEATERS

XXXVIII - DETERMINATION OF THERMAL PERFORMANCE OF RECTANGULAR- AND TRAPEZOIDAL-SHAPED INNER-SKIN PASSAGES FOR ANTI-ICING SYSTEMS

By L. M. K. Boelter, V. D. Sanders, and F. E. Romie

SUMMARY

The results of an experimental determination of the thermal and hydrodynamic behavior of air in the downstream portion of two types of double-skin passages used in heated-air leading-edge anti-icing systems are presented.

Local heat-transfer rates and static-pressure drops were measured for small ducts of trapezoidal and rectangular cross section. These ducts were used to simulate the heat-transfer characteristics of the inner skin of anti-icing heated wings. The range of Reynolds moduli for the tests was from 1000 to about 10,000.

The measured unit thermal conductances were plotted as a function of Reynolds modulus and as a function of the distance from the leading edge of the heated test plate. Results for both the trapezoidal and rectangular ducts indicated that the downstream average unit thermal conductance in the turbulent region was 30 to 35 percent below that given by the commonly used equations. In the laminar region, the experimental unit conductance was found to be approximately 30 percent below predicted values for the rectangular ducts but for the trapezoidal ducts the data were much lower than the predicted values.

Temperature measurements of the inner skin indicated that it acted as a highly effective fin. This was corroborated by calculations in which the inner skin was considered to be a fin.

INTRODUCTION

Values of the unit thermal conductance for air flowing inside the double-skin passages must be known in order to design a heated-air, leading-edge, anti-icing system.

Most of the available data on the thermal conductances for flow of air inside ducts concern the values at points far downstream from the duct entrance. (Reference 1, however, contains values of the local thermal conductance near the entrance of a circular tube.) Data which define the local heat-transfer rate throughout the length of heated straight ducts are presented herein.

A steam-condensing calorimetric test section containing long, straightened ducts, typical of double-skin passages used in the leading-edges of airfoils was designed and constructed. Two types of inner skin using trapezoidal- and rectangular-shaped passages have been tested. Data required to obtain values of the unit thermal conductance were recorded as a function of distance along the passages in order to study the behavior of the air in the downstream region.

The following data were obtained:

(1) Local steam condensation rates, which are proportional to heat-transfer rates

(2) Inlet- and outlet-air temperatures

(3) Various surface temperatures of steam plate and inner skin

(4) Weight rates of air passing through test section

(5) Local and over-all static-pressure drops

This investigation, part of a research program conducted on anti-icing systems at the University of California, was sponsored by and conducted with the financial assistance of the National Advisory Committee for Aeronautics.

SYMBOLS

A	heat-transfer area of inner and outer skins, square feet
A_x	cross-sectional area of duct, square feet

B	duct width, feet
b	number of duct passages (10)
c_p	unit heat capacity, Btu/(lb)($^\circ$F)
D_H	hydraulic diameter, feet $\left(4A_x/P\right)$
ΔF	frictional pressure loss, (lb)/(sq ft)
f_c	unit thermal convective conductance (based on logarithmic-mean temperature difference), Btu/(hr)(sq ft)($^\circ$F)
f_{c_x}	local unit thermal conductance, Btu/(hr)(sq ft)($^\circ$F)
G	weight rate of fluid per unit of cross-sectional area, (lb)/(hr)(sq ft)
g	gravitational force per unit of mass, (lb)/(lb-sec^2)/(ft)
h	heat of evaporation of 1 cubic centimeter of water at atmospheric pressure, Btu/(cc)
k	thermal conductivity of air, Btu/(hr)(sq ft)($^\circ$F/ft)
L	total length of duct passage, feet
l	width of condensate section (length of duct traversing one condensate section), feet
Nu	Nusselt modulus, dimensionless $\left(f_c D_H/k\right)$
P	wetted perimeter of duct passage, feet
Pr	Prandtl modulus, dimensionless $\left(\frac{\mu c_p(3600g)}{k}\right)$
q	rate of heat transfer, Btu/(hr)
R	steam condensation rate obtained under "load" conditions, (cc)/(hr)
R_o	steam condensation rate obtained under "no-load" conditions, (cc)/(hr)

Re	Reynolds modulus, dimensionless $\left(GD_H/3600g\mu\right)$
t_p	mean temperature of duct wall for section m, ^oF
u	mean air velocity, (ft)/(sec)
W	air weight rate through all duct passages, (lb)/(hr)
x	distance from duct entrance, feet
γ	weight density of air, (lb)/(cu ft)
δ	thickness of rectangular duct, feet
ζ	isothermal friction factor defined by $\frac{\Delta F}{\gamma} = \zeta \frac{L}{D_H} \frac{u^2}{2g}$
μ	absolute viscosity, (lb)(sec)/(sq ft)
τ	air temperature, ^oF
τ_o	temperature of air entering ducts, ^oF
τ_m	average mixed mean temperature of air in section m, ^oF

Subscripts:

av	average
m	mth condensate section

DESCRIPTION OF APPARATUS

The test stand used for the experimental work in this investigation is shown in figure 1. The test stand consisted of three parts: (1) The steam chest, (2) the inner-skin inserts, and (3) the burette chamber. The apparatus was constructed so that various inner skins could be attached to the heated plate, thereby simulating the double-skin passages employed in heated-air leading-edge systems.

The heated plate was an integral part of the steam chest, which was a machined casting. The air side of the plate was polished and contained studs to allow the double-skin inserts to be attached by means of wing nuts. Precautionary measures were taken to assure good thermal bond along the contact area of the insert and the heated plate.

The details of the steam chest are shown in figures 2 and 3. Eleven condensate collecting sections were used to measure the local values of unit thermal conductance. For each particular section, the amount of heat transferred from the steam to the air in the double-skin passages was measured by the condensate collected in a thermally insulated glass burette. The steam for all runs was at a pressure of about 1 inch of mercury above atmospheric pressure.

Thermocouples were placed at several points along the inserts and the heated plate. A traversing thermocouple was placed at the entrance section of the ducts to measure the entering air temperature. The exit-air temperature was measured by three thermocouples embedded at equal intervals in a 1/8-inch-diameter copper bar placed across the length of the duct exits. An orifice plate with a long 1/8-inch slit of the same length as the copper bar was placed between the bar and the duct exits in order to insure mixing for measurement of the mixed mean temperature.

Pressure taps were located at four points in each of two passages. These taps allowed the measurement of local values of static pressure.

Air at room temperature was drawn into the test section and was metered by means of a sharp-edged orifice and pipe taps in a 2-inch pipe.

The thermal performance of two types of double-skin passages was investigated. Both double skins were made of 0.032-inch aluminum sheet and when attached to the heated plate formed 10 air passages. The first insert was trapezoidal in cross section (fig. 2) and was similar to the type described in reference 2. The second unit was constructed of a flat aluminum sheet placed over 1/4-inch-square brass rods, which formed the separation for the air passages (fig. 2). With certain modifications in the arrangements described above, the effects of a thermal contact resistance for the trapezoidal section and the fin effect of the inner skin of the rectangular section were demonstrated.

ANALYSIS OF DATA

Analysis of the steam condensation data was accomplished in the following manner. "No-load" data were obtained when air was not allowed to enter the duct passages. The no-load data thus represent that amount of heat which was lost through the burette tubes and the insulation surrounding the ducts. It was a heat loss which occurred whether or not air was flowing in the duct passages and was therefore subtracted from the condensation rate obtained under "load" conditions.

Thus, the heat transferred from the mth condensate section to the air flowing through the passages is

$$q_m = h\left(R_m - R_o\right)$$

where h is the heat of evaporation of 1 cubic centimeter of water at steam-chest conditions in British thermal units per cubic centimeter, R_m is the load rate of condensation in cubic centimeters per hour, and R_o is the no-load condensation rate in cubic centimeters per hour. The increase in temperature of the air flowing over this section is

$$\Delta\tau = \frac{q_m}{Wc_p}$$

and the temperature of the air at the center of each section (i.e., the average air temperature for that section) is given by

$$\tau_m = \tau_o + \sum_{n=1}^{n=m-1}\left(\frac{q_n}{Wc_p}\right) + \frac{q_m}{2Wc_p}$$

where τ_o is the temperature of the air at the entrance to the duct, W is the weight rate of air through the 10 air passages in pounds per hour, and c_p is the heat capacity of the air in British thermal units per pound per ^oF.

The value of the average unit thermal conductance for section m is thus

$$f_{c_m} = \frac{q_m}{bPl_m\left(t_p - \tau_m\right)}$$

where b is the number of passages (10), P is the duct perimeter in feet, l_m is the width of the condensate section in feet, and t_p is the mean of the inner- and outer-skin-surface temperatures of the duct in section m. Measurements of the duct temperature of the inner skin indicated that the temperature was very nearly equal to the temperature of the steam plate (212^o F). Thus the fin effectiveness of the inner skin was experimentally determined to be very large. The high fin effectiveness of the inner skin was also corroborated by calculations.

More rigorous calculation would require that the local temperature difference used in calculating f_{c_m} should be the logarithmic-mean temperature difference for each condensate section. However, the temperature of the air passing along each condensate section does not increase sufficiently to make a significant difference between the local logarithmic-mean temperature difference and the local arithmetic-mean temperature difference.

The mean value, with respect to length, of the local unit conductance calculated in this report is to be used with the over-all logarithmic-mean temperature difference when calculating over-all heat-transfer rates.

Heat balances were obtained by dividing the measured enthalpy change of the air by the heat supplied by the condensing steam. Heat balances for the trapezoidal sections averaged 1.06 with a minimum value of 1.02 and a maximum value of 1.26 (obtained for the lowest rate). Heat balances for the rectangular ducts averaged 1.18 with a minimum value of 0.95 and a maximum value of 1.38.

RESULTS AND DISCUSSION

Heat Transfer

The unit thermal conductance, plotted as a function of distance from the duct entrance, is presented in figures 4(a) and 4(b) for rectangular ducts and trapezoidal ducts, respectively. Data obtained from condensate sections 7 and 11, corresponding to points 9.5 and 24 inches from the duct entrance, respectively, are omitted from these figures. Data from section 7 are omitted because of condensate leakage from the condensate section to the surrounding steam chest. Section 11 served the function of a guard section to eliminate end conduction errors and was thus not used.

For trapezoidal ducts (fig. 4(b)), the unit thermal conductance attains a constant value at a point 6 inches (or 25 hydraulic diam) from the duct entrance. It is usually found that the unit conductance becomes constant after approximately 5 to 10 hydraulic diameters from the entrance (references 1 and 3 to 5). There are insufficient data to determine whether this large difference in "entrance lengths" is due to defects in the experimental apparatus or to the effects of the geometry of the duct cross section. The scatter of the data points in this region near the entrance for both the trapezoidal and rectangular ducts may be due to the construction of the test apparatus.

The values of Nusselt modulus, averaged with respect to length, are plotted against Reynolds modulus in figure 5. The data for the turbulent region for both trapezoidal and rectangular ducts fall on the same line. In the turbulent region these values lie about 30 percent below the line given by the equation $Nu = 0.022Re^{0.8}Pr^{0.33}$ (reference 6). Data summarized in reference 7 for air flowing in rectangular ducts are about 10 to 15 percent below the data given by this equation.

For Reynolds moduli less than about 1700, the data for rectangular ducts are approximately 20 percent below the predicted curve in figure 5. The predicted curve for the laminar region is obtained from the equation (reference 6, pp. 43 and 44):

$$Nu_{av} = \frac{f_{c_{av}} D_H}{k} = 7.6 \frac{1}{L} \int_0^L \left(1 + \frac{1}{59} \frac{Wc_p}{kx} \frac{\delta}{B}\right)^{1/3} dx$$

This equation is an integrated mean value of the expression for the local or point unit thermal conductance. For the magnitudes of W, δ, B, and L considered here the above expression is within 30 percent of the simpler equation

$$Nu_{av} = 7.6$$

stated in reference 8. The values of the unit thermal conductance in the present report are based on the logarithmic-mean temperature potential.

Transition from laminar to turbulent flow for rectangular ducts, as indicated by the heat-transfer data, occurs at $Re = 1700$ and is also shown in the plot of static-pressure drop against weight rate for the rectangular ducts (fig. 6(a)). However, data for the trapezoidal ducts do not show transition from turbulent to laminar flow either in the curve of Nu against Re (fig. 5) or in the curve of pressure drop against weight rate (fig. 6(b)). (Similar results were found in the tests reported in reference 9.) The cause of this phenomenon is not apparent but two items may be considered. The data for the trapezoidal duct were not taken for Reynolds moduli of less than 1300. Also, the geometry of the trapezoidal duct may retard transition from the turbulent to the laminar regime; that is, the transition may occur at a lower value of the Reynolds modulus.

The inner skin increases the heat transferred to the outer skin by means of the "fin effect" of the inner skin. The fact that the inner skin is very effective as a fin was demonstrated by measurement of the inner-skin temperature, which was within 10° F of the outer-skin

temperature over the range of air weight rates for which the data were obtained. A further study of this fin effect was made upon the replacement of the brass (k = 70Btu/(hr)(sq ft)($^{\circ}$F/ft)) spacer strips (fig. 2) by Bakelite (k $\approx$ 0.1 Btu/(hr)(sq ft)($^{\circ}$F/ft)) strips of the same size. From figure 7 it may be seen that this substitution decreased the heat rate for the weight rate chosen by approximately 20 percent at the duct entrance. The difference between the two curves decreases with increasing distance from the tube entrance because the temperature difference of the air and duct wall necessarily becomes greater in the downstream region when Bakelite spacers are used.

The reduction in heat transfer which occurs when a thermal contact resistance exists between the inner and outer skins of a heated wing has been calculated and shows that for f_c = 6 Btu/(hr)(sq ft)($^{\circ}$F), the heat transfer for the trapezoidal sections should be decreased by about 20 percent if a thermal contact resistance equivalent to an air gap of 0.006 inch exists between the inner and outer skins. Experimental results showed that the decrease in heat transferred when a 0.0053-inch paper strip was inserted between the inner and outer skins was less than 20 percent. Thus it may be concluded that the method of attachment of the inner skin is of relatively minor importance.

Pressure Drop

The static-pressure-drop data for both isothermal and nonisothermal flow in rectangular and trapezoidal ducts are presented in figure 6. The static taps used in obtaining these data were both within the duct passage (equal cross-sectional areas); therefore the static-pressure drop for isothermal flow is also the total-pressure drop for isothermal flow. Four static taps were provided in each of two duct passages. These taps were spaced $1\frac{1}{2}$, 6, 18, and 25 inches from the duct entrance. Plots at constant weight rate of the static pressure against length of passage gave, in all cases, straight lines so that only the data from two static taps (i.e., the difference in static pressure between the two taps) are presented.

It can be observed that the nonisothermal pressure drop is increased by approximately 50 percent over the isothermal pressure drop. This difference is about twice as much as would be predicted by means of the equations given in reference 10. The reason for the large difference is not apparent.

The isothermal static-pressure drop (fig. 6(a)) in the laminar region for rectangular ducts varies as the 1.2 power of the weight rate. It is well-established both analytically and experimentally for circular tubes that the exponent should be 1.0 in the laminar region.

The friction factor plotted against Reynolds modulus for rectangular and trapezoidal ducts is given in figure 8. Excellent agreement between experimental and predicted values is obtained for trapezoidal ducts. The friction factor for the rectangular ducts varies from about 15 percent below the predicted value at Re = 2000 to about 27 percent below the predicted value at Re = 10,000.

CONCLUSIONS

From an investigation of the thermal performance of rectangular- and trapezoidal-shaped inner-skin passages for anti-icing systems, the following conclusions are drawn:

1. In the turbulent region, the average unit thermal conductance for both the trapezoidal and rectangular ducts is about 35 percent less than the values obtained from commonly used equations.

2. Heat-transfer and pressure data obtained for the trapezoidal duct over a range of Reynolds moduli between 1300 and 16,000 indicate that the flow was turbulent.

3. Data obtained for rectangular ducts reveal that the flow may be laminar at values of Reynolds modulus below 1800. Examination of the local heat-transfer rates indicates that the flow may be laminar near the entrances of the double-skin passages even for large values of Reynolds modulus.

4. Measurements of the temperature of the inner-skin surfaces indicate that the inner skin is effective in transferring heat to the outer skin and that perfect bonding of the two surfaces is not necessary.

5. Isothermal pressure drops are predictable within about 20 percent.

6. Additional data should be obtained to establish the effect of various types of entrance (such as are used in actual systems) on the heat-transfer and pressure-drop characteristics of the double-skin passages.

Department of Engineering,
University of California,
Berkeley, Calif., March 26, 1946

REFERENCES

1. Boelter, L. M. K., Young, G., and Iversen, H. W.: An Investigation of Aircraft Heaters. XXVII - Distribution of Heat-Transfer Rate in the Entrance Section of a Circular Tube. NACA TN 1451, 1948.

2. Neel, Carr B., Jr.: An Investigation of a Thermal Ice-Prevention System for a C-46 Cargo Airplane. I - Analysis of the Thermal Design for Wings, Empennage, and Windshield. NACA ARR 5A03, 1945.

3. Boelter, L. M. K., Leasure, R., Romie, F. E., Sanders, V. D., Elswick, W. R., and Young, G.: An Investigation of Aircraft Heaters. XXXIII - Experimental Determination of Thermal and Hydrodynamical Behavior of Air Flowing along Finned Plates. NACA TN 2072, 1950.

4. Boelter, L. M. K., Sanders, V. D., Young, G., Morgan, M., and Morrin, E. H.: An Investigation of Aircraft Heaters. XXXIV - Experimental Determination of Thermal and Hydrodynamical Behavior of Air Flowing between a Flat and a Wave-Shaped Plate. NACA TN 2426, 1951.

5. Boelter, L. M. K., Young, G., Greenfield, M. L., Sanders, V. D., and Morgan, M.: An Investigation of Aircraft Heaters. XXXVII - Experimental Determination of Thermal and Hydrodynamical Behavior of Air Flowing along a Flat Plate Containing Turbulence Promotors. NACA TN 2517, 1951.

6. Boelter, L. M. K., Martinelli, R. C., Romie, F. E., and Morrin, E. H.: An Investigation of Aircraft Heaters. XVIII - A Design Manual for Exhaust Gas and Air Heat Exchangers. NACA ARR 5A06, 1945.

7. Drexel, Roger E., and McAdams, William H.: Heat-Transfer Coefficients for Air Flowing in Round Tubes, in Rectangular Ducts, and around Finned Cylinders. NACA ARR 4F28, 1945.

8. Norris, R. H., and Streid, D. D.: Laminar-Flow Heat-Transfer Coefficients for Ducts. Trans. A.S.M.E., vol. 62, no. 6, Aug. 1940, pp. 525-533.

9. Boelter, L. M. K., et al.: Analysis of Heat and Mass Transfer Mechanisms of Thermal Anti-Icing Systems. Rep. to Air Technical Service Command Ice Research Base, Univ. of Calif., Sept. 1945.

10. Boelter, L. M. K., Morrin, E. H., Martinelli, R. C., and Poppendiek, H. F.: An Investigation of Aircraft Heaters. XIV - An Air and Heat Flow Analysis of a Ram-Operated Heater and Duct System. NACA ARR 4C01, 1944.

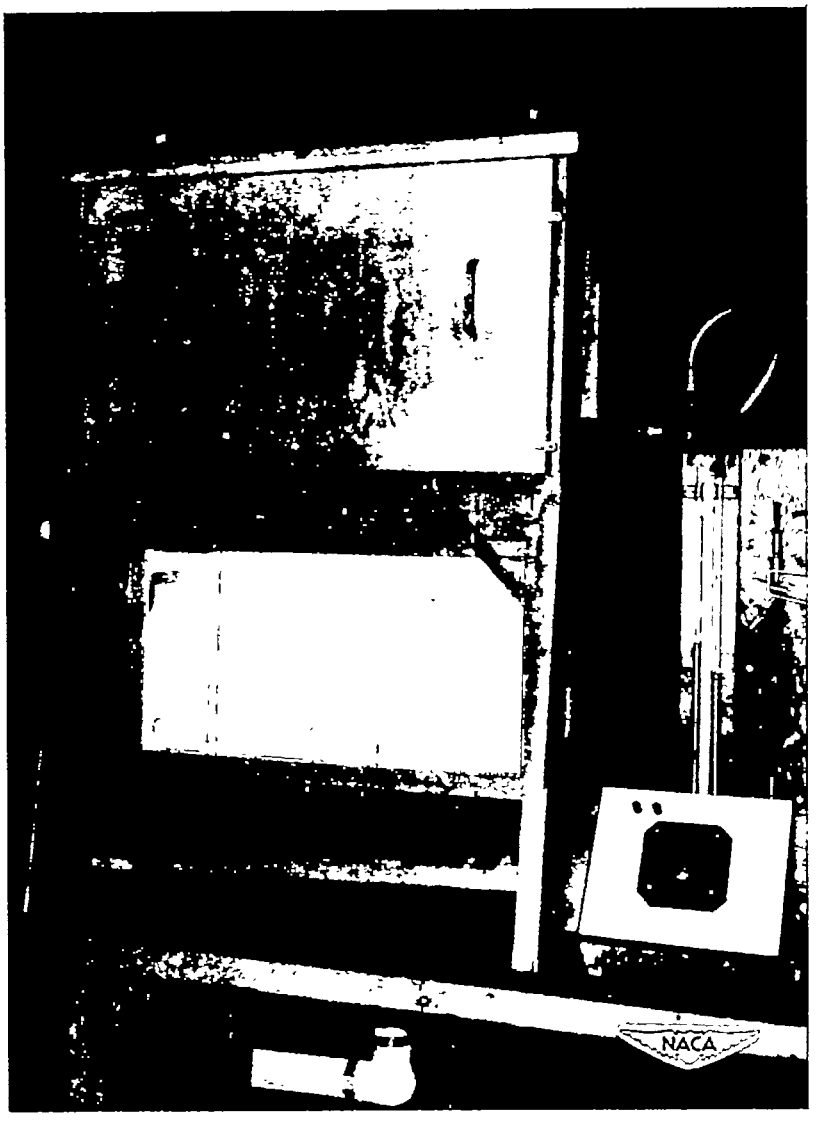

Figure 1.- Apparatus with steam chest and condensate section shown above burette chamber. Air enters test section through bellmouth slit at right.

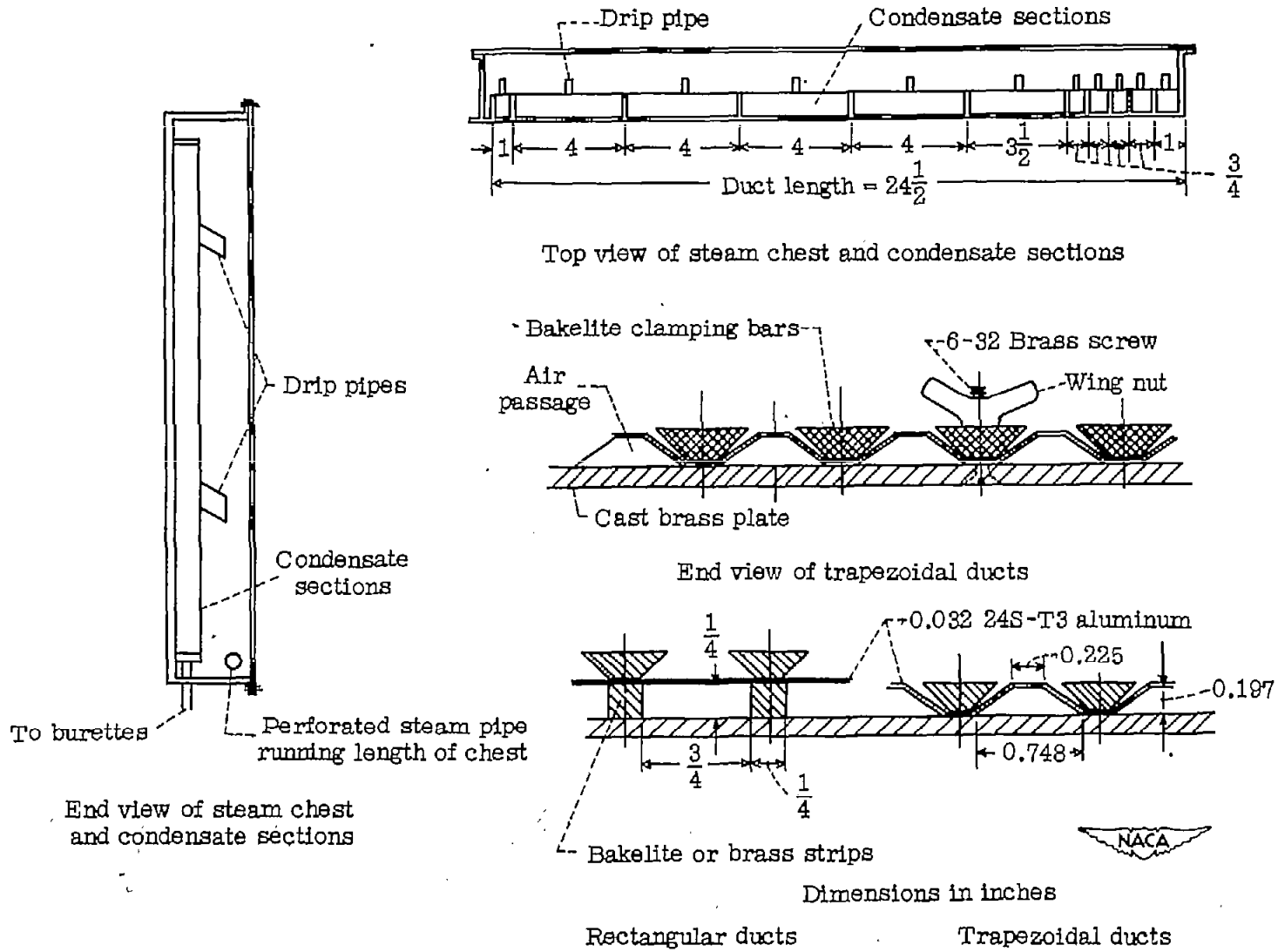

Figure 2.- Details of test apparatus.

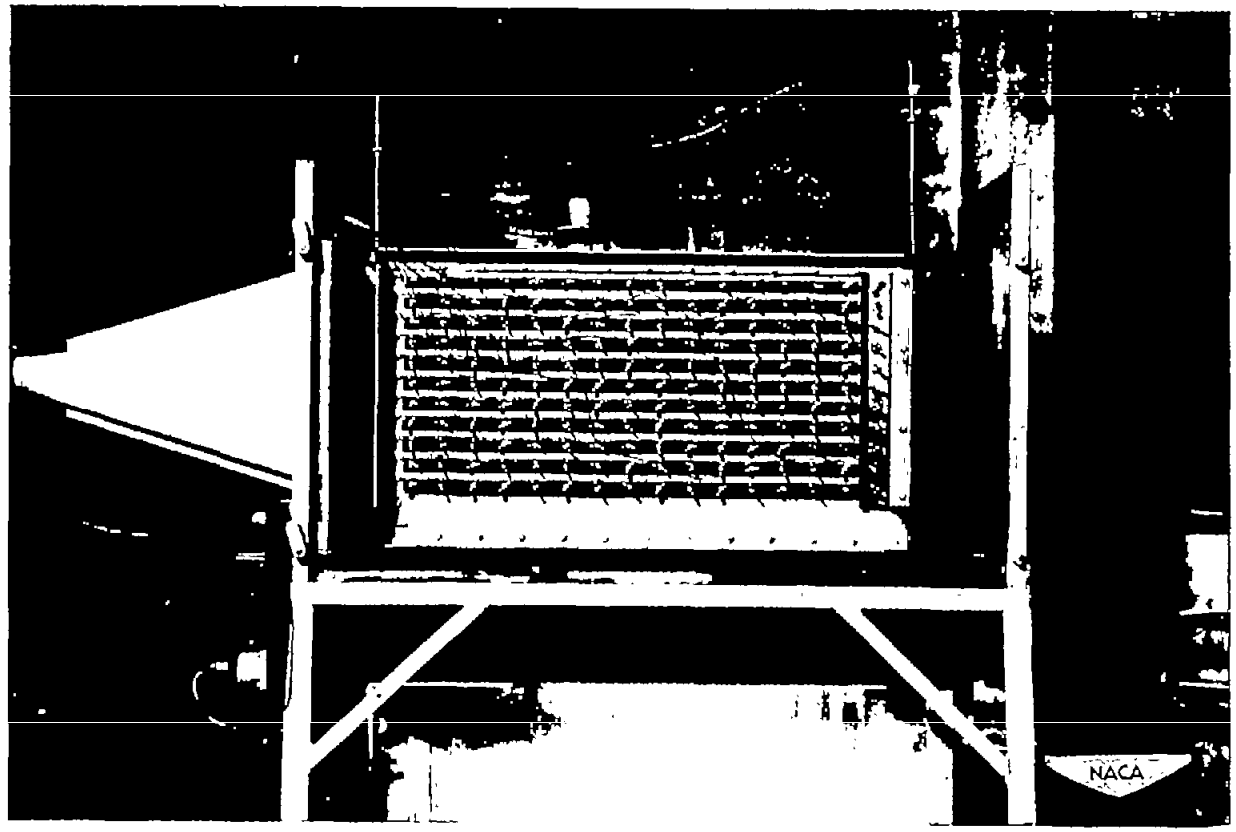

Figure 3.- Method of attachment of trapezoidal-shaped inner skin to steam-heated plate.

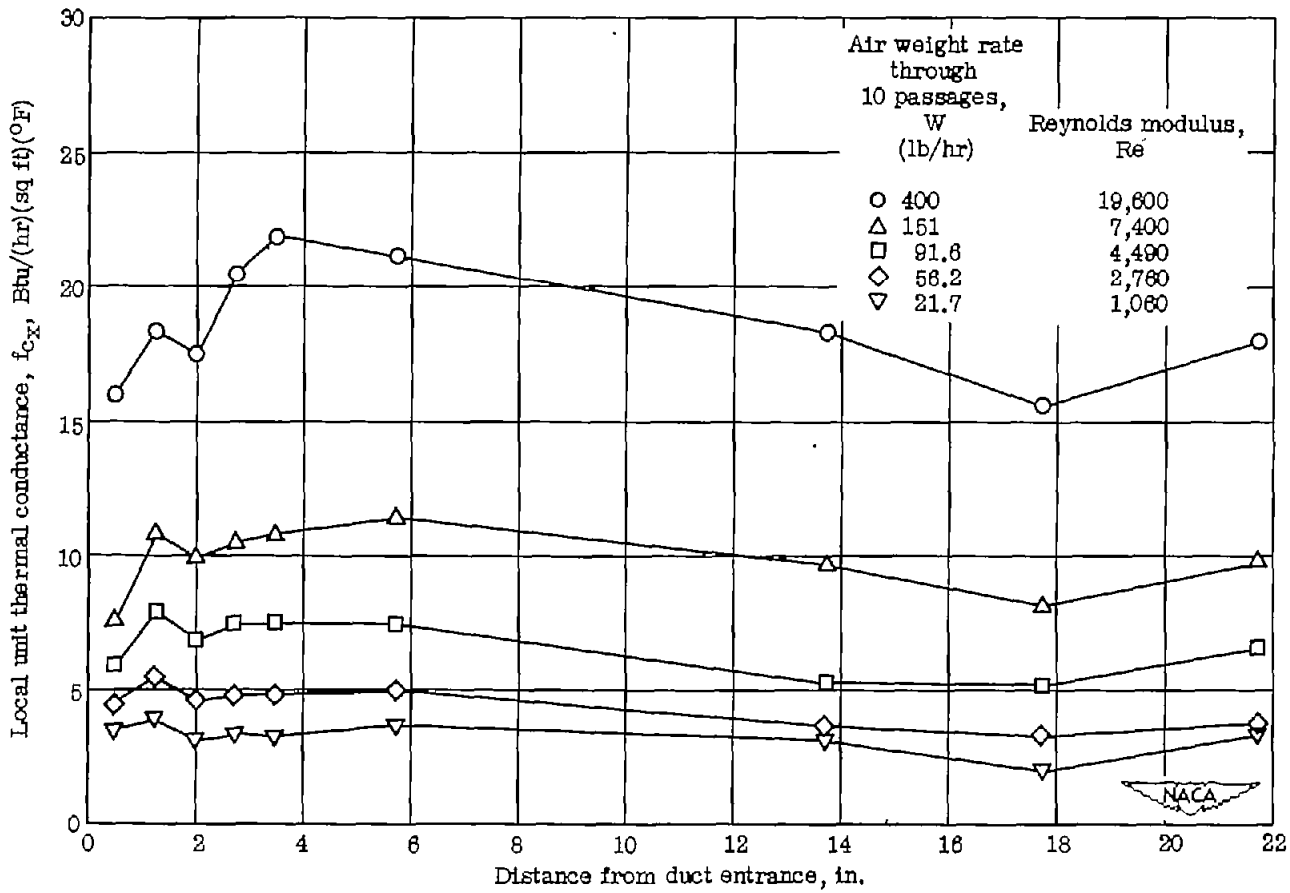

(a) Rectangular ducts.

Figure 4.- Variation of local unit thermal conductance with distance from duct entrance.

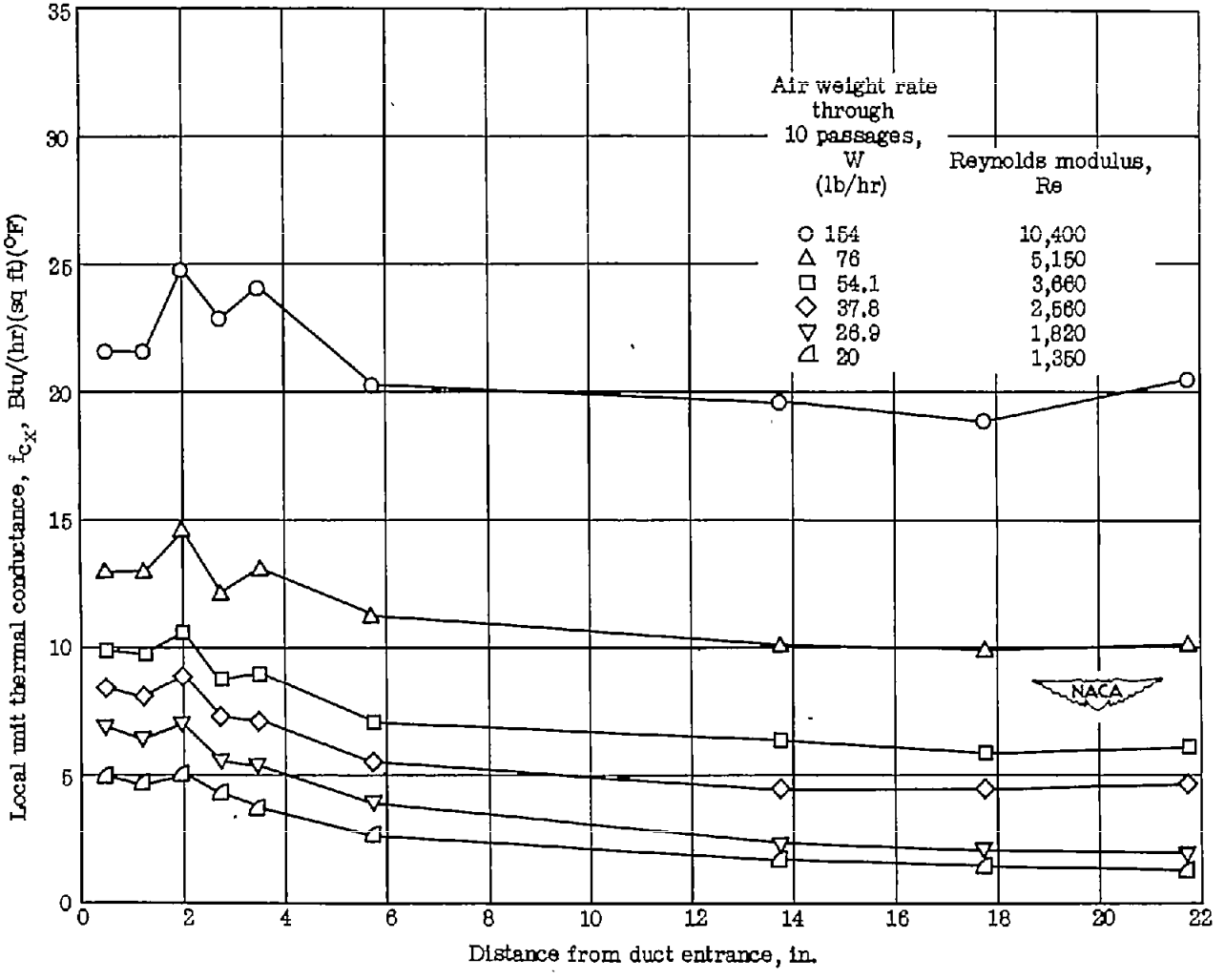

(b) Trapezoidal ducts.

Figure 4.- Concluded.

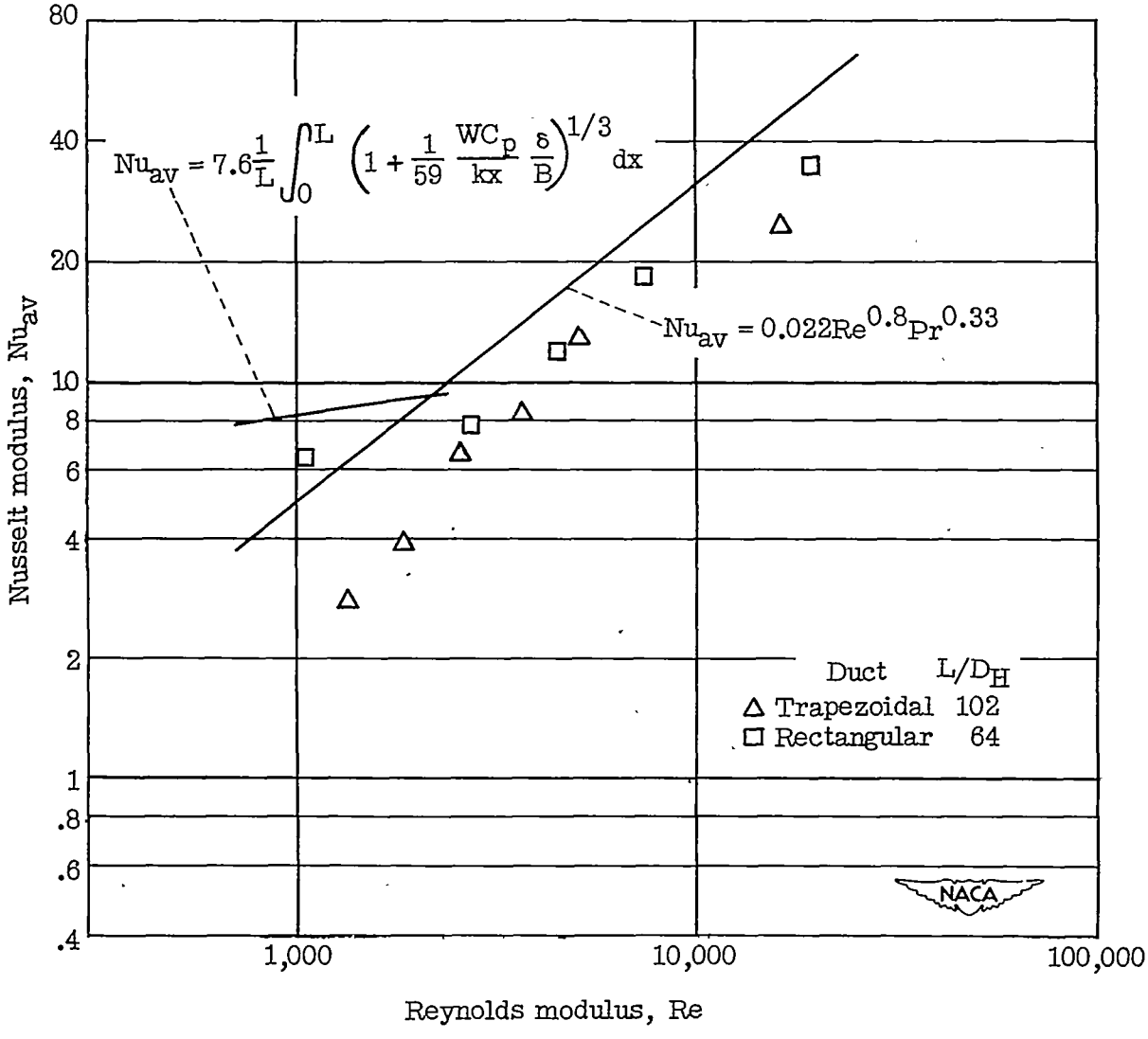

Figure 5.- Variation of Nusselt modulus with Reynolds modulus for rectangular and trapezoidal ducts.

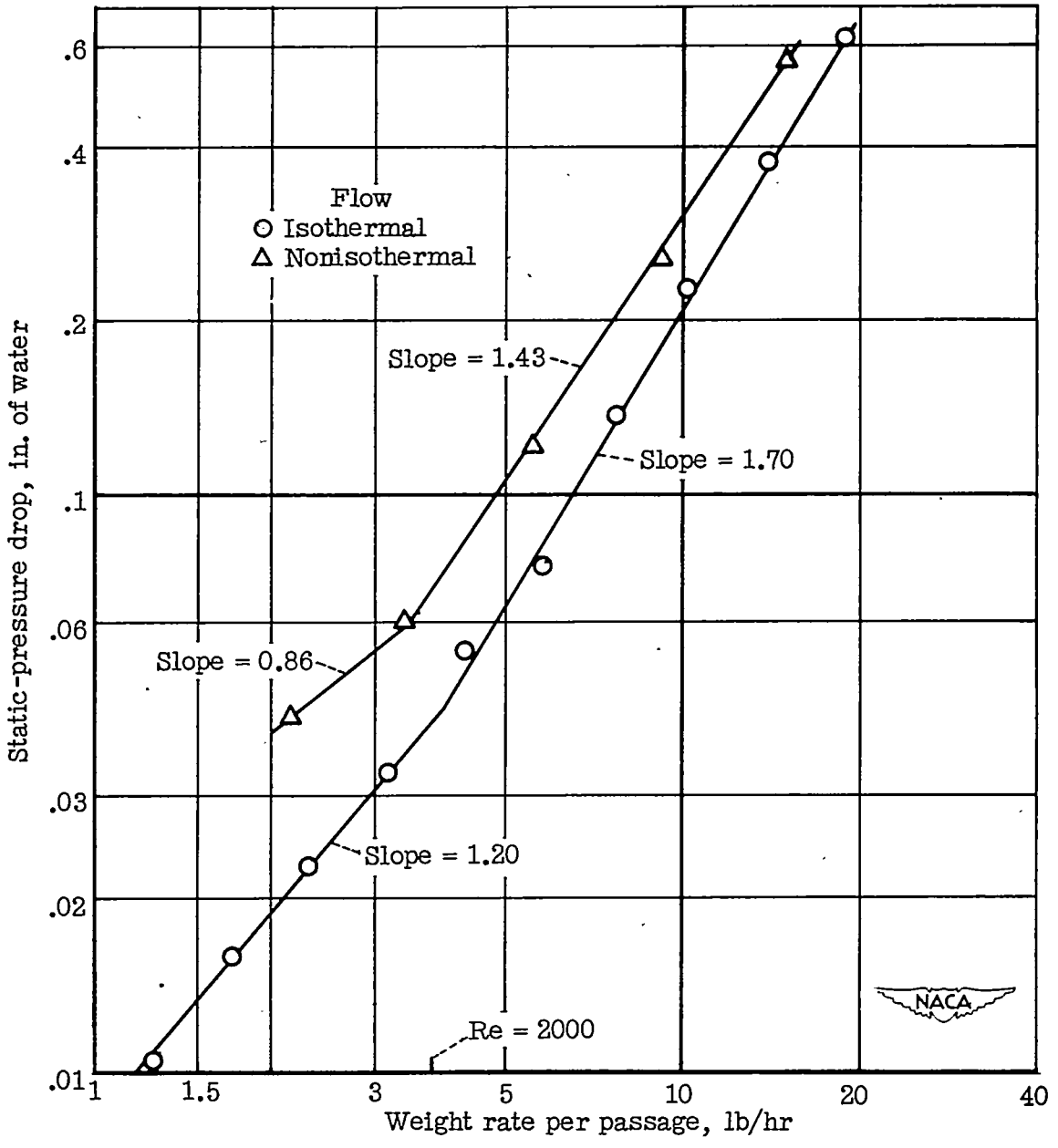

(a) Rectangular ducts.

Figure 6.- Variation of static-pressure drop with weight rate. First static tap 6 inches from duct entrance; 19 inches between static taps; entering air temperature, approximately 65° F.

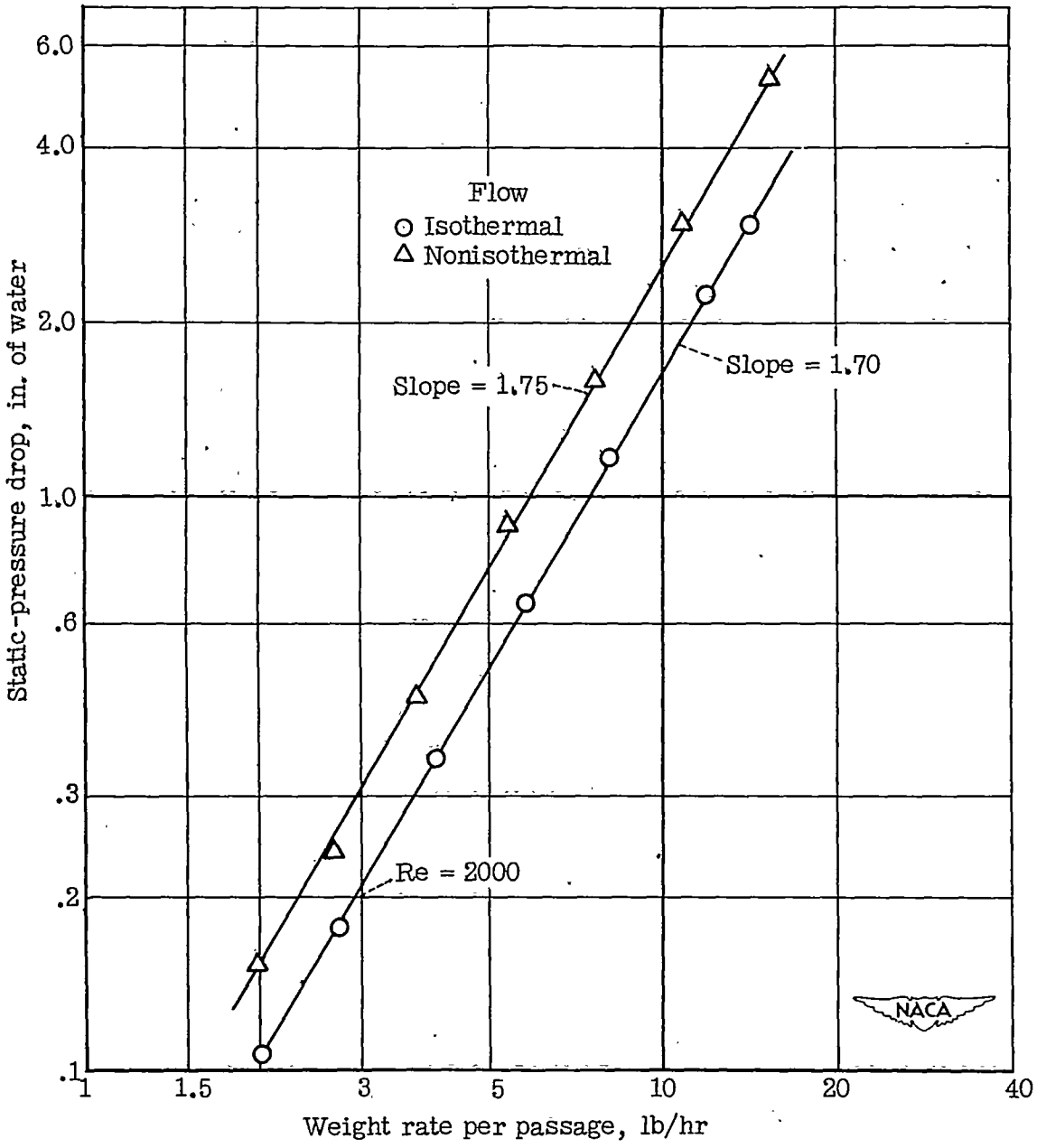

(b) Trapezoidal ducts.

Figure 6.- Concluded.

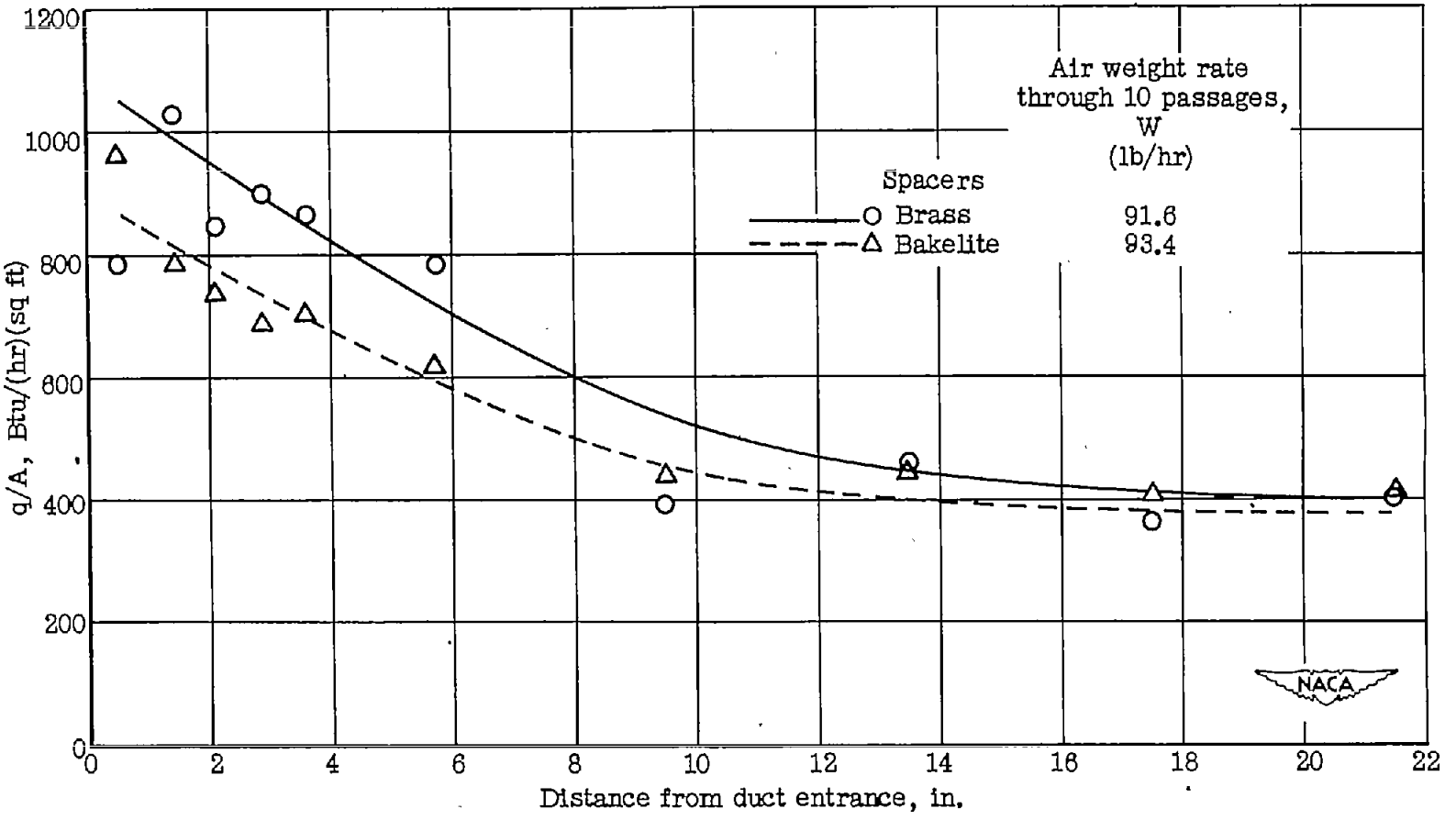

Figure 7.- Effect of thermal resistance between inner and outer skins of rectangular ducts.

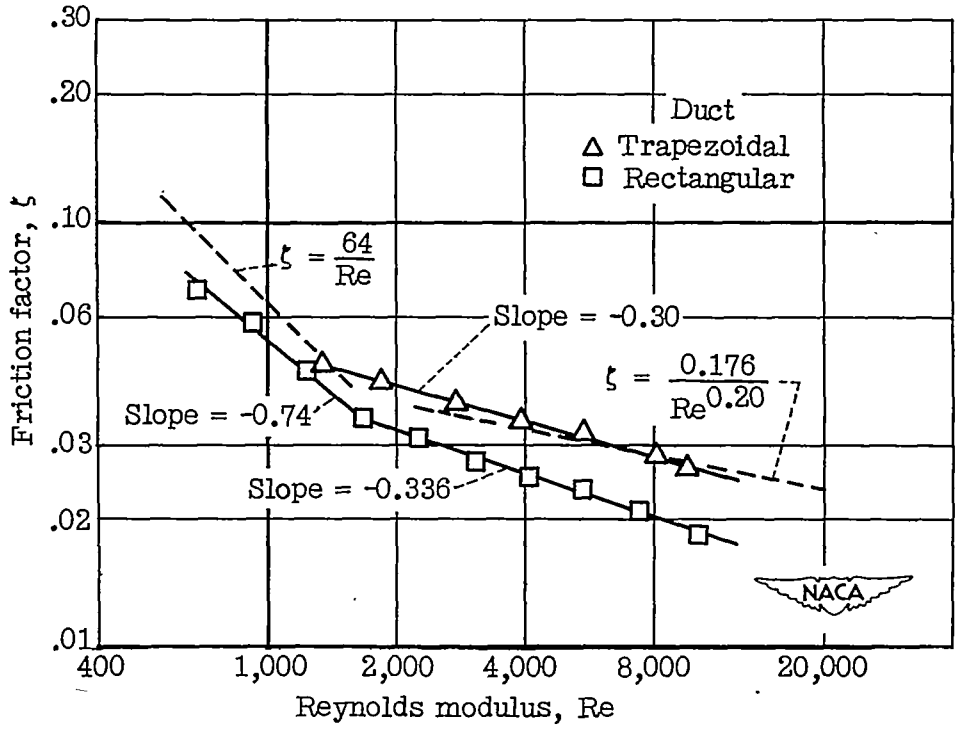

Figure 8.- Variation of friction factor with Reynolds modulus for isothermal flow.

NACA-Langley - 11-2-51 - 1000